Subcentimeter depth resolution using a single-photon counting time-of-flight laser ranging system at 1550 nm wavelength

Ryan E. Warburton,[1] Aongus McCarthy,[1] Andrew M. Wallace,[1] Sergio Hernandez-Marin,[1] Robert H. Hadfield,[2] Sae Woo Nam,[2] and Gerald S. Buller[1,*]

[1]School of Engineering of Physical Sciences, Heriot-Watt University, Riccarton, Edinburgh, EH14 4AS, UK
[2]Optoelectronics Division 815, National Institute of Standards and Technology, Boulder, Colorado 80305, USA
*Corresponding author: G.S.Buller@hw.ac.uk

Received March 28, 2007; accepted May 30, 2007;
posted June 21, 2007 (Doc. ID 81603); published July 30, 2007

We demonstrate subcentimeter depth profiling at a stand off distance of 330 m using a time-of-flight approach based on time-correlated single-photon counting. For the first time to our knowledge, the photon-counting time-of-flight technique was demonstrated at a wavelength of 1550 nm using a superconducting nanowire single-photon detector. The performance achieved suggests that a system using superconducting detectors has the potential for low-light-level and eye-safe operation. The system's instrumental response was 70 ps full width at half-maximum, which meant that 1 cm surface-to-surface resolution could be achieved by locating the centroids of each return signal. A depth resolution of 4 mm was achieved by employing an optimized signal-processing algorithm based on a reversible jump Markov chain Monte Carlo method.

OCIS codes: 280.3640, 030.5260, 040.0040.

Light detection and ranging (LIDAR) is a well-established technique for both distance metrology and remote sensing. A number of optical methods have been developed to measure distance based on triangulation, interferometry, or time-of-flight [1]. Coherent LIDAR has also been used to measure range and velocity [2] and has been further enhanced by the use of optical frequency combs [3]. This Letter describes new developments in a time-of-flight system using time-correlated single-photon counting (TCSPC). TCSPC is a measurement technique that combines high detection sensitivity with picosecond timing resolution and has applications in, for example, time-resolved photoluminescence and quantum key distribution [4]. Time-of-flight depth measurement based on TCSPC has been investigated for a number of years in the context of three-dimensional (3D) imaging and laser scanning [5,6]. The technique provides ranging information using low average power lasers and lends itself to eye-safe operation and applications that require the recognition of objects from their surface topology (i.e., range profiling). Much of our earlier work [5,6] investigated the 3D modeling of macroscopic objects under laboratory conditions at ranges of several meters since the technique can achieve depth resolutions of tens of micrometers when large numbers (typically $\sim 10^6$) of single-photon returns are recorded. In later work, the technique has been used at distances greater than 1 km for the detection and analysis of distributed targets, i.e., those containing more than one scattering surface [7]. TCSPC has also been used to construct 3D images using arrays of semiconductor single-photon detectors [8] and single-photon counting microchannel plates with crossed delay lines [9].

Most previous work on distributed targets using a time-of-flight approach has been performed using single-photon avalanche diode (SPAD) detectors, particularly those fabricated with silicon, which limits the operational wavelength to less than 1 μm. Previously, thick-junction Si SPADs with a jitter of approximately 400 ps FWHM [10] were used in conjunction with a laser operating at a wavelength of 630 nm to achieve a minimum resolvable surface-to-surface separation of 1.7 cm using optimized signal processing algorithms (see below). SPADs operating in the 1550 nm wavelength region are based on reduced bandgap semiconductors and offer inferior performance to their Si counterparts. For example, InGaAs/InP SPADs have detection efficiencies greater than 10% at 1550 nm, but suffer from high

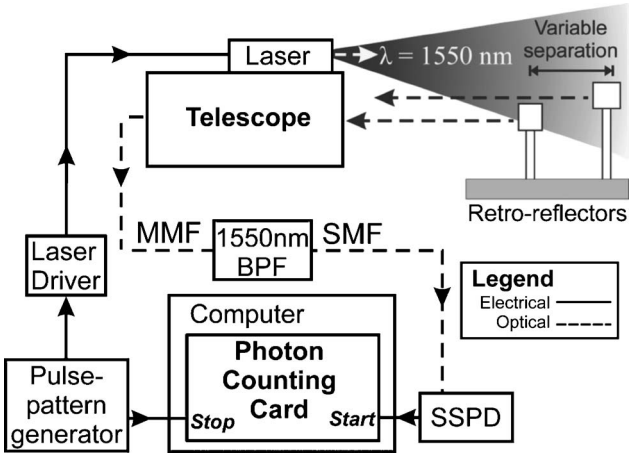

Fig. 1. System schematic (BPF=bandpass filter, MMF=multimode fiber, SMF=single-mode fiber). The pulse pattern generator provides the synchronization signal for the laser and provides a (delayed) electrical trigger signal to stop the timing sequence. A photon event returned from the target starts the timing sequence, and the time difference between start and stop is recorded on a PC-based data acquisition card. Examples of distributions of these time differences are shown in the histogram in Fig. 2.

dark count rates and the deleterious effects of afterpulsing, which generally result in a need for both gated operation and much reduced overall count rates [11] compared with Si-based SPADs. In this Letter we present ranging results obtained with a nanopatterned superconducting single-photon detector (SSPD), which has demonstrated single-photon sensitivity at longer wavelengths with lower jitter of 68 ps FWHM and a Gaussian profile [12]. We estimate the minimum resolvable surface separation using the same approach employed previously [10]. The data from these measurements were processed using two different algorithms (described below) in order to determine the surface-to-surface separation. The minimum resolvable separation was 4 mm.

The SSPD is a 100 nm wide niobium nitride wire patterned in a meander line covering a 10 μm $\times$10 μm area [13]. The SSPD is fiber-packaged and mounted in a cryogen-free, commercial cryocooler [14] operating at a temperature of 3 K. The detector is mounted on a stage with passive temperature stabilization, and the fiber coupling is not affected by cryocooler vibrations. The detector is coupled via a single-mode telecommunications fiber to the rest of the optical ranging system. This type of detector offers several important advantages: single-photon sensitivity at infrared wavelengths ($\sim$1% detection efficiency at $\lambda \sim 1550$ nm), coupled with low timing jitter ($<$70 ps), short recovery time ($<$10 ns), and low dark counts ($<$100 counts per second). With the SSPDs used in this Letter, we were able to utilize a pulsed laser emitting at 1550 nm, resulting in a ranging system that is more eye-safe. The main contribution to the background count level in the measurement is from ambient light; however, this is reduced by spectral, spatial, and temporal filtering [7]. Operation at the 1550 nm wavelength, as described in this Letter, allows these filtering techniques to be applied with much greater efficacy, as the solar background is greatly reduced at this wavelength, making the system considerably more robust against changes in the ambient light level.

The transceiver (Fig. 1) comprises a standard 200 mm diameter aperture telescope with a 1550 nm wavelength pulsed laser diode (pulse FWHM less than 50 ps). The eyepiece of the telescope was modified for imaging onto a CCD camera for initial alignment and for the collection of the reflected laser signal, which is focused into a multimode optical fiber. An in-line bandpass interference filter (FWHM $\sim$15 nm) centered at a wavelength of 1550 nm was used to reduce the background light at the detector. All measurements were taken during ambient daylight conditions with an average laser power of $\sim$5 μW. A pulse-pattern generator (operated at 40 MHz) was used to clock the laser driver and synchronize the signal for data acquisition.

To determine the surface-to-surface separation, two identical air-filled retroreflecting corner cubes were attached to translation stages and mounted on an optomechanical rail that was positioned at a range of approximately 330 m from the telescope. The retroreflectors were used to provide two closely spaced reflecting surfaces with variable separation from 500 mm down to a minimum of 1 mm. The optics of the laser diode were configured so that both corner cubes were illuminated at the range of 330 m, and the photon returns were collected by the telescope.

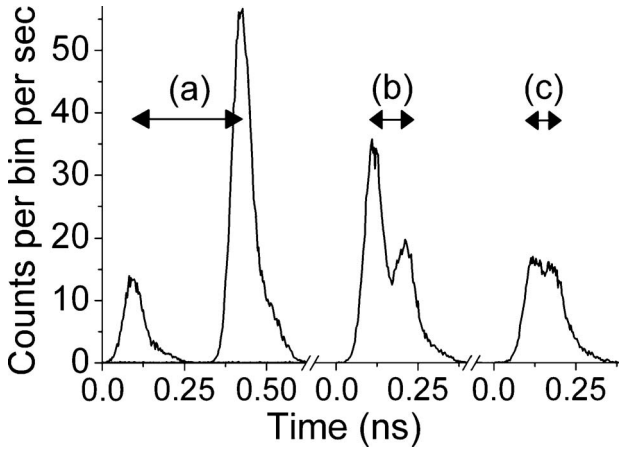

Fig. 2. Three separate examples of the time responses of the system where the target consisted of two corner-cube retroreflectors separated by (a) 50, (b) 15, and (c) 10 mm. The acquisition time was 30 s in each case. The heights of each trace are slightly different due to variations in optical alignment among the three measurements.

In Fig. 2 we see three typical photon-return histograms as recorded by the photon-counting card. In this example the corner cubes were separated by a distance of 50 mm in Fig. 2(a), 15 mm in Fig. 2(b), and 10 mm in Fig. 2(c). An acquisition time of 30 s was used in each case. In these examples, the 4096 channels, or bins, of the photon-counting card were divided over 12.5 ns, giving a bin width of 3.073 ps. Photon returns were recorded at a rate of $\sim$1000/s (dependent on the optical alignment). In Fig. 2, the instrument response of each surface return is 70 ps FWHM; the slight shoulder on the right-hand side of each individual surface return is due to the asymmetric shape of the laser output pulse.

To analyze the results, two different approaches were implemented. The first method is straightforward: the position of each peak is determined by its centroid from which the surface separation can be estimated. This is a satisfactory approach for well-separated return peaks; however, as the two surface return signals merge, the process becomes increasingly problematic.

For peak separations that overlap, we used a previously developed algorithm based on reversible jump Markov chain Monte Carlo (RJMCMC) techniques [15]. This technique determines an estimate of the number of scattering surfaces, their positions, and the amplitudes of the returned signals from a distributed target. The RJMCMC approach is an extension of the basic Markov chain Monte Carlo (MCMC) algorithm designed to allow jumps between different solutions with different numbers of surface scatterers. Therefore, it is possible to consider the number of peaks as an unknown. In these experiments the only *a priori* information that we include is

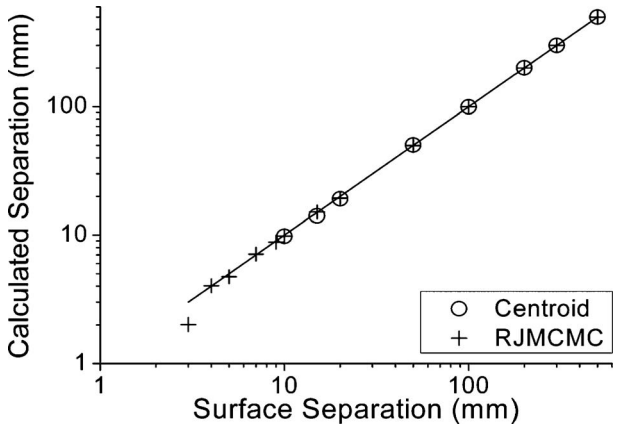

Fig. 3. Calculated separation versus surface separation. An acquisition time of 30 s was required for each data point; photon returns were recorded at a rate of ~1000/s. The black line represents the case of perfect agreement.

the instrumental response of the detector. We initialized RJMCMC with ten uniformly distributed peaks to represent our lack of knowledge about the actual distribution of the target return. We are able to extract the positions and amplitudes of the returned signals from appropriate prior distributions, as explained in [16].

Figure 3 shows the separation calculated using both centroid and RJMCMC methods. At large separations both processes perform well. For surface separations of less than 10 mm the target returns were sufficiently close to render the centroid method wholly unreliable. However, it is clear that using the RJMCMC algorithms enables a much lower separation to be resolved, 4 mm being the minimum reliably demonstrated with these measurements.

We have successfully demonstrated subcentimeter ranging resolution at a standoff distance of 330 m at a wavelength of 1550 nm using time-correlated single-photon counting with a superconducting niobium nitride nanowire single-photon detector. This low jitter detector, used in conjunction with advanced signal processing algorithms, has permitted depth resolution in the millimeter range for the first time to our knowledge using this ranging technique. Furthermore, operation in the 1550 nm spectral region enables eye-safe ranging to be carried out in daylight conditions.

We thank QinetiQ, Malvern for previously funded work, and SELEX for its support with algorithm development. S. W. Nam and R. H. Hadfield acknowledge support from the DARPA QuIST program and the NIST Quantum Information Science initiative, and also thank Gregory Gol'tsman for supplying the original detectors used in this work. The authors acknowledge useful discussions with Robert Lamb, SELEX.

References

1. M.-C. Amann, T. Bosch, R. Myllyla, and M. Rioux, Opt. Eng. **40**, 1019 (2001).
2. C. J. Karlsson, F. Å. A. Olsson, D. Letalick, and M. Harris, Appl. Opt. **39**, 3716 (2000).
3. W. C. Swann and N. R. Newbury, Opt. Lett. **31** (2006).
4. W. Becker, in *Advanced Time-Correlated Single Photon Counting Techniques*, Vol. 81 of Springer Series in Chemical Physics (Springer, 2005).
5. J. S. Massa, A. M. Wallace, G. S. Buller, S. J. Fancey, and A. C. Walker, Opt. Lett. **22**, 543 (1997).
6. A. M. Wallace, G. S. Buller, and A. C. Walker, Comput. Control Eng. J. **12**, 157 (2001).
7. G. S. Buller, R. D. Harkins, A. McCarthy, P. A. Hiskett, G. R. MacKinnon, G. R. Smith, R. Sung, A. M. Wallace, K. D. Ridley, J. G. Rarity, and R. A. Lamb, Rev. Sci. Instrum. **76**, 083112 (2005).
8. M. A. Albota, R. M. Heinrichs, D. G. Kocher, D. G. Fouche, B. E. Player, M. E. O'Brien, B. F. Aull, J. J. Zayhowski, J. Mooney, B. C. Willard, and R. R. Carlson, Appl. Opt. **41**, 7671 (2002).
9. C. Ho, K. L. Albright, A. W. Bird, J. Bradley, D. E. Casperson, M. Hindman, W. C. Priedhorsky, R. Scarlett, R. C. Smith, J. Thieler, and S. K. Wilson, Appl. Opt. **38**, 1833 (1999).
10. R. E. Warburton, A. McCarthy, A. M. Wallace, S. Hernandez-Marin, S. Cova, R. A. Lamb, and G. S. Buller, Opt. Express **15**, 423 (2007).
11. S. Pellegrini, R. E. Warburton, L. J. J. Tan, J. S. Ng, A. Krysa, K. Groom, J. P. R. David, S. Cova, M. J. Robertson, and G. S. Buller, IEEE J. Quantum Electron. **42**, 397 (2006).
12. M. J. Stevens, R. H. Hadfield, R. E. Schwall, S. W. Nam, R. P. Mirin, and J. A. Gupta, Appl. Phys. Lett. **89**, 031109 (2006).
13. A. Verevkin, J. Zhang, R. Sobolewski, A. Lipatov, O. Gkhunev, G. Chulkova, A. Korneev, K. Simrov, G. N. Gol'tsman, and A. Semenov, Appl. Phys. Lett. **80**, 705 (2002).
14. R. H. Hadfield, M. J. Steven, S. G. Gruber, A. J. Miller, R. E. Schwall, R. P. Mirin, and S. W. Nam, Opt. Express **13**, 10846 (2005).
15. S. Richardson and P. J. Green, J. R. Stat. Soc. Ser. B **59**, 731 (1997).
16. S. Hernandez-Marin, A. M. Wallace, and G. J. Gibson, in *IAPR Conference on Machine Vision Applications* (Springer-Verlag, 2005).